Title

A systematic solution to quantify economic values of vehicle grid integration

Authors

Zhang, Haifeng
Tian, Ming
Zhang, Cong
et al.

Publication Date

2021-10-01

DOI

10.1016/j.energy.2021.121006

A Systematic Solution to Quantify Economic Values of Vehicle Grid Integration

Haifeng Zhang[a], Ming Tian[a], Cong Zhang[b]*, Bin Wang[b] and Dai Wang[c]

a School of Mechanical and Automotive Engineering, Shanghai University of Engineering Science, No. 333 Longteng Rd., Shanghai 201620, China

b Lawrence Berkeley National Laboratory, 1 Cyclotron Rd., Berkeley, CA 94720, United States

c Tesla Inc., 3500 Deer Creek Rd, Palo Alto, CA 94304, USA

Highlights

• An integrated framework is developed to quantify values of VGI.

• The proposed predictive algorithm greatly enhances the real-time allocation performance.

• Optimization models reduce system costs in both wholesale and retail markets.

Abstract

Vehicle-Grid-Integration (VGI) supplies one of the potential benefit extensions for electric vehicles (EVs) to make use of their parking time, which enables the EVs to provide grid services while still meeting consumer driving needs. However, the costs, benefits and risks of VGI still remain unclear, which limits the development of the VGI to promote the interaction between the EV and grid. In this study, we propose an integrated framework to quantify and utilize the aggregate flexibility of the EVs to supply the grid services in electricity markets. The integrated solution includes five sub-modules that cover end-to-end functionalities from individual EV energy consumption

estimation to final monetary values calculation of providing grid services. Both wholesale market and local level charging management are formulated in the optimization module. A predictive control algorithm is proposed to allocate power to individual vehicles in real time, considering uncertainties from dispatch signal and travel behavior. Simulation results from 10,000 EVs indicate that the proposed optimization methods can significantly reduce the system cost in both wholesale market and retail market. Local tariff optimization reduces the electricity cost by 24.4% compared to uncontrolled charging. Wholesale market optimization results show that $691 and $255 revenues can be captured by each EV in ERCOT and CAISO markets per year, although with a conservative assumption on battery throughput cost at 0.16$/kWh.

Keywords: vehicle-grid-integration; electric vehicle; simulation platform; real-time allocation

Nomenclature

Indices

i EVs index, $i = 1, 2, \ldots, I$

t Time index, $t = 1, 2, \ldots, T$

Parameters

ε Battery degradation cost, in $/kWh

Δt Time step, in hour

$\lambda(t)$ Electricity price (Time-of-use rate) in retail market at time *t*, in $/kWh

$\omega(t)$ Energy conversion ratio of reserve at time *t*, in %

$\sigma(t)$ Energy conversion ratio of frequency regulation at time *t*, in %

$Price^{down}(t)$ Frequency regulation down price in day ahead market at time *t*, in $/kW

$Price^{up}(t)$ Frequency regulation up price in day ahead market at time *t*, in $/kW

$Price^{energy}(t)$ Energy price in day ahead market at time *t*, in $/kWh

$Price^{reserve}(t)$ Reserve price in day ahead market at time *t*, in $/kW

Variables

$\overline{e_i}$ Upper bound of cumulative energy of EV *i*, in kWh

$\underline{e_i}$ Lower bound of cumulative energy of EV *i*, in kWh

$\overline{E}$ Upper bound of aggregate cumulative energy of EV fleet, in kWh

$\underline{E}$ Lower bound of aggregate cumulative energy of EV fleet, in kWh

$\overline{p_i}$ Upper bound of power of EV *i*, in kW

$\underline{p_i}$ Lower bound of power of EV *i*, in kW

$\overline{P}$ Upper bound of aggregate power of EV fleet, in kW

$\underline{P}$ Lower bound of aggregate power of EV fleet, in kW

$\alpha(t)$ Binary variable, 1 if the battery is discharging in day ahead market, 0 otherwise

$\beta(t)$ Binary variable, 1 if the battery is charging in day ahead market, 0 otherwise

SOE(t) State of energy of aggregated battery at time t, in kWh

$E^b(t)$ Energy bought in day ahead market at time *t*, in kWh

$E^s(t)$ Energy sold in day ahead market at time *t*, in kWh

$F^{down}(t)$ Frequency regulation down capacity bought in day ahead market at time *t*, in kW

$F^{up}(t)$ Frequency regulation up capacity sold in day ahead market at time *t*, in kW

$R(t)$ Reserve capacity sold in day ahead market at time *t*, in kW

1. Introduction

Transportation electrification is one of critical paths to achieve deep greenhouse emission reduction targets [1][2]. Moving towards this goal, California government has recently updated the zero-emissions vehicle (ZEV) mandate, which targets to launch as many as 5 million ZEVs by 2030 [3][4]. Previous studies have proven that the electric vehicles (EVs) can satisfy majority of daily travel requirements of the US drivers [4][5][6][7][8]. In the meantime, cars are parked nearly 95% of time, which allows the vehicle batteries to support grid objectives such as renewable energy integration [9][10].

As of 2020, there were over 5.5 million EVs globally [11], with numbers expected to dramatically increase in coming years. U.S. states are setting ambitious EV targets, such as the ten-state Zero Emission Vehicle Alliance [12] and according to forecasts from EVAdoption, the EV sales share in 2028 will reach 18% [13]. More broadly, a similar increase in EV is occurring in Europe, with transportation electrification projections potentially requiring an added 4% of electricity generation capacity by 2030 [14] [15].

This growth in EV sales will inevitably have a large impact on electricity load and grid integration [16]. Therefore, utilities and regional transmission organizations (RTOs) are beginning to investigate the impact of EVs on their systems [17].

From the grid perspective, there is a low capital cost of grid storage using vehicles (capital cost is absorbed for mobility objectives), yet the grid services from vehicles can be used to lower the operating costs for EV owners[18]. In this manner, a synergy exists where flexibility in EV charging can provide valuable grid support on various scales of aggregation, from behind-the-meter tariff optimization [19][20][21], to distribution systems support [22], to wholesale market support with ancillary services [23][24]. Despite these opportunities, it is still unclear whether "vehicle-grid-integration" (VGI) is feasible in terms of its costs, values risks, complexity, and whether it is competitive with other technologies that can offer similar grid services.

In order to quantify the monetary benefits of VGI, many researchers proposed different strategies to integrate the flexibility of EVs into electricity market (both retail and wholesale markets)[25][26]. Among these studies, there are mainly two methods to model the flexible resource from EV. The first method is to integrate the individual EV into the whole aggregator's optimization model. Then solving the whole problem will not only provide aggregate power commitment (e.g. day-ahead bids), but also return the detailed charging/discharging schedule for each individual EV. Sortomme et al. proposed a novel V2G algorithm to optimize the service and energy scheduling[27]. This methodology maximizes the profits to the aggregator while supplying the peak load

shaving ability and extra system flexibility to the grid system and minimize the EV charging cost to the customer. Vagropoulos et al. came up with a novel bidding algorithm for regulation services to maximize the flexible energy in the system[28]. Mehta et al. presented two smart charging algorithms that considered the existing infrastructure of the distribution system, in order to minimize the peak-to-valley ratio and the whole system cost[29]. The work listed above provides a comprehensive understanding on EVs' contribution to ancillary services, however, there are still two outstanding questions: (1) how to cope with the uncertainty of individual EV in both real-time and day-ahead markets. (2) how to make computational time affordable if the EV number is large and time resolution is high (e.g. 1 or 5 min). Even though some researchers developed distributed algorithms to handle the computational time bottleneck [30][31], it would bring new problems like communication delay and convergence.

The second way is to model the aggregator's optimization based on flexibility aggregation. The aggregator firstly quantifies the total flexibility of a population of EVs. All EVs together are regarded as one "virtual battery". Only constraints of the "virtual battery" are built into the optimization problem, rather than information of individual vehicles. Thus, it can significantly reduce the computational burden. After getting the aggregate power commitments, the aggregator will disaggregate the total power into individual vehicles at service liquidation time. In this way, the uncertainties from vehicle side and dispatch signal from power system will be handled at real time stage. However, a key challenge is to estimate the aggregate flexibility of the EV fleet. The aggregate

flexibility depends on exogenous stochastic processes such as arrival/departure, maximum power rates and charging demands. Researchers in proposed a method to evaluate the capacity of Vehicle-to-Grid (V2G) for an individual vehicle [32]. However, the scalability of proposed model is limited, so we cannot directly use it to evaluate the flexibility of a population of EVs. In [33][34], the authors studied the potential of EVs on enhancing the renewable penetration. The flexibility was modeled according to the consumption increasing of renewable energy. This study only considered the single direction charging and required deterministic information from EVs. Authors in [35] estimated the influence on the grid system flexibility when the V2G fleet attended the regulation market. The Markov process was used to predict the V2G capacity of the EVs, with the precondition of meeting the daily energy need by scheduling the charge and discharge operations. However, the charge/discharge behaviors change the battery state of energy and furthermore influence the V2G capacity. In [36], the authors proposed a method to estimate the aggregate V2G fleet flexibility. Aggregated parameters are used to describe the power and energy constraints and reduce forecast errors. However, there is no clue how to calculate the minimum energy demand, which is a key parameter in the aggregate model[37]. In literature [38][39][40], integrated systems between the PV and existing household grid system are investigated to decrease the system cost, which is focusing on the microgrid level. Our previous work also investigates the integration between the EVs and the system grid, which shows a strong impacts on the system load reshape at a macro level [41][42].

To address above questions and concerns, we developed an integrated simulation framework. Firstly, individual EV model is established to estimate the state of charge, energy consumption, battery degradation, and etc. Then an aggregate model is used to evaluate the aggregate flexibility from a collection of EVs based on individual vehicle information. With the aggregate flexibility, we model both retail and wholesale market level optimization problems to calculate the benefits that can be obtained by providing grid services. A model predictive control (MPC) method is developed to allocate total power into individual vehicles in a distributed manner, considering the randomness from travel behavior and dispatch signals from power systems. The contributions of this paper are mainly four-folds:

1) An integrated framework is proposed to quantify the feasibility of VGI. The simulation platform is highly modularized. It allows researchers and scholars to plug their own modules (e.g. bidding strategy, real-time dispatch algorithm) and get holistic solutions;

2) A bottom-up method is implemented to quantify the aggregate flexibility of a population of EVs. Detailed vehicle model is built to precisely estimate individual vehicle parameters such as energy consumption, state-of-charge for battery;

3) Local tariff optimization and wholesale market optimization models are formulated to capture values from different markets. Values are stacked to maximize the benefits from VGI. It should be noted that the optimization results heavily depend

on market factors such as market bidding timeline, price volatility, market products, etc. The goal of this paper is to provide a framework to evaluate VGI values, instead of beating certain existing benchmarks.

4) An MPC-based method is deployed to disaggregate total charging/discharging into individual vehicles considering the uncertainties from vehicle behavior and dispatch signals.

2. Simulation framework

The proposed framework includes five sub-modules as shown in Figure 1. They are EV Estimation Module, Capacity Availability Module, Delivery Optimization Module, Resource Allocation Module and Value Estimation Module.

In EV Estimation Module, vehicle travel itineraries and driving cycles are taken as inputs to model individual vehicle status including state-of-charge, current input/output, battery health, etc. The energy constraint and power constraint of each vehicle are also modeled at this stage. For the sake of estimating the capability of vehicles to supply the local and grid services, we aggregate the collection of EVs and model them as a single "virtual battery" in the Capacity Availability Module. This module generates aggregate level constraints and sends them to Delivery Optimization Module. The objective of the Delivery Optimization Module is to determine both grid and local service portfolios that can be offered to maximize the total economic benefits. The aggregator can commit to provide either local service or wholesale market service by comparing the benefits from

these two markets. Also, by solving the optimization problems, the aggregator is able to submit the day-ahead bids to the system operator if it decides to provide wholesale market services. Then the system operator will clear the market and reward the aggregator at market clearing prices. Since the Delivery Optimization Module only generates aggregate level commitments, the total charging/discharging power should be allocated to individual EVs afterwards. In the meantime, the system operator will forward the dispatch signals to aggregators (e.g. AGC signal, deployment signal for spinning reserve, etc.). However, there are uncertainties from dispatch signals and EV behaviors. In particular, the resource allocation module will decide in the real-time operations: (1) which EVs population is chosen to be scheduled charging/discharging; (2) what is the scheduled charging/discharging power of each vehicle. After performing delivery optimization and resource allocation, all the awards and penalties will be liquidated. The Value Estimation Module will calculate the benefits and costs of different stakeholders including EV owners, aggregator, utility company and etc. We will elaborate on each module in Section 4.

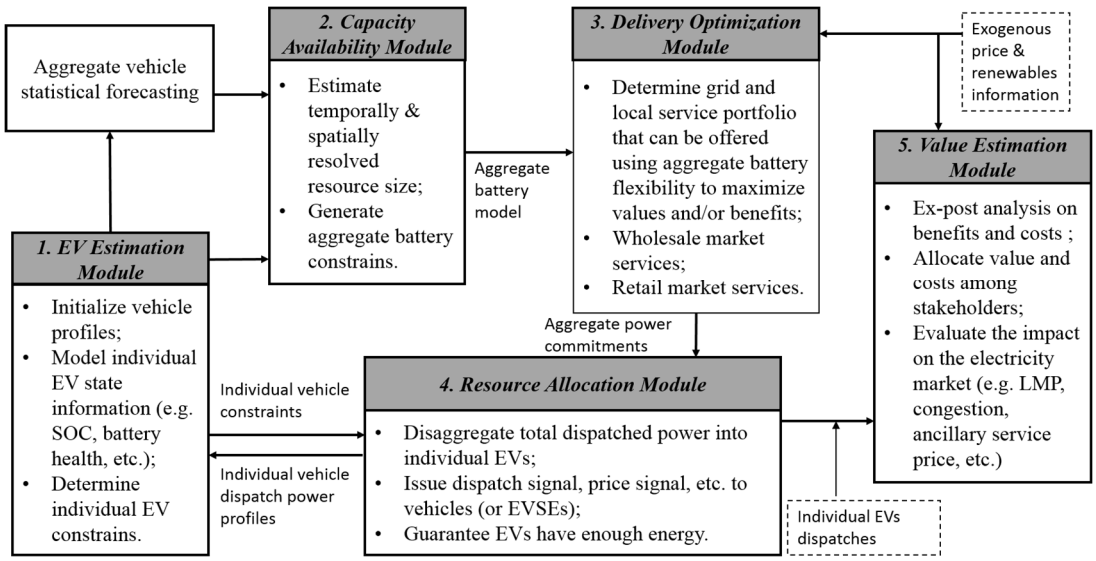

Figure 1. Simulation framework.

3. Description of sub-modules (Modeling)

3.1. EV Estimation Module

The structure of EV Estimation Module is shown in Figure 2. In this section, vehicle travel profile is regarded as a collection of events (parking and driving). The travel itineraries can be either generated from statistics or the real-world dataset. Table 1 shows a typical daily travel itinerary.

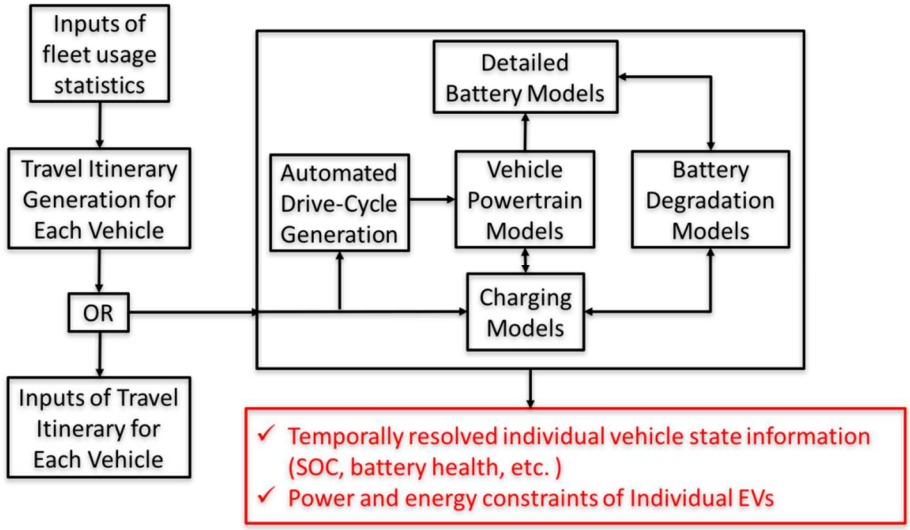

Figure 2. Framework of EV Estimation Module.

Table 1. A travel itinerary example

Begin time	End time	Length	stop
0:00	7:25	0	Home
7:25	8:00	22	Driving
8:00	17:00	0	work
17:00	18:30	25.0	Driving
18:30	19:10	0	Shopping
19:10	19:50	10	Driving
19:50	24:00	0	Home

In this work, we develop a powertrain model, which is similar to the models of Autonomie [43]. This model is adopted to predict the energy consumption of EVs on any

trip-specific driving cycle, and with any level of ancillary power loading (e.g. HVAC system). When the vehicle is driving, it tracks temperature, energy consumption, SOC, current, open circuit voltage and other parameters. Three Environmental Protection Agency (EPA) driving cycles [44], including highway (HWFET), urban dynamometer driving schedule (UDDS), and aggressive driving(US06), are used to represent the different driving types in this paper. Powertrain simulation results like current, open circuit voltage and temperature, are also used to calculate battery degradation.

Detailed battery degradation model can be found in our previous publication [45]. The battery degradation is divided into two parts: calendar life loss and cycle life loss. Calendar life loss is a function which is related to the temperature and time, while the cycle life loss is related to current rate, cumulative throughput and temperature.

$$D_{\text{CycleLoss}} = (\xi \cdot Temp^2 + \psi \cdot Temp + \zeta) \exp[(\upsilon \cdot Temp + \theta) \cdot S_{\text{rate}}] \cdot Ah_{\text{Through}} \tag{1}$$

$$D_{\text{CalendarLoss}} = f \cdot \exp[-J_{\text{ac}} / (G \cdot L_{\text{day}})] \cdot L_{\text{day}}^{1/2} \tag{2}$$

$$D_{\text{Loss}} = D_{\text{CycleLoss}} + D_{\text{CalendarLoss}} \tag{3}$$

where $(\xi \cdot Temp^2 + \psi \cdot Temp + \zeta)$ and f are pre-exponential factors, $Temp$ is the absolute temperature, $\xi / \psi / \zeta / \upsilon / \theta$ are fitted from curve, S_{rate} is the current C rate, Ah_{Through} represents the amount of charge delivered by the battery during cycling, L_{day} is the days, J_{ac} is the activation energy in J mol^{-1}, G is the gas constant. These parameters values are listed in the Table 2.

Table 2. Parameter value of the battery degradation

Parameter	Value	Parameter	Value
ξ	8.61×10^{-6}, 1/Ah-K^2	S_{rate}	C-Rate
ψ	-5.13×10^{-3}, 1/Ah-K	L_{day}	Days
ζ	7.63×10^{-1}, 1/Ah	J_{ac}	24.5, kJ·mol^{-1}
ι	-6.7×10^{-3}, 1/K-(C-rate)	G	8.314, J·mol^{-1}·K^{-1}
ϵ	2.35, 1/(C-rate)	*Temp*	K
f	14,876, 1/day1/2	-	-

We can see from equation (1) that battery degradation is a complex non-linear function of temperature, current and total throughput. In the following optimization models, we assume that battery works at constant temperature and current, so the battery degradation is simplified to be a linear function of battery total throughput. However, the detailed models (1) –(2) presented above can still be used in different use cases which need more in-depth modeling of battery degradation.

With different charging models/configurations, we can get the temporally resolved information on individual EV status. The charging power and energy of individual EVs will be used in the capacity availability module to estimate the aggregate flexibility of a population of EVs.

3.2. Capacity Availability Module

Considering a collection of EVs, we have access to their arrival and departure statistics from historical data archives, as well as drivers' inputs on desired departure time and charging demands [46]. We can define a default or nominal charging profile for each EV. Each of these EVs is flexible such that they can accept perturbations around this nominal charging profile. They can get charged immediately at maximum charge rate right after plug-in or defer the charge for a time period. These EVs are indifferent to charging profiles as long as their net demand is met before departure.

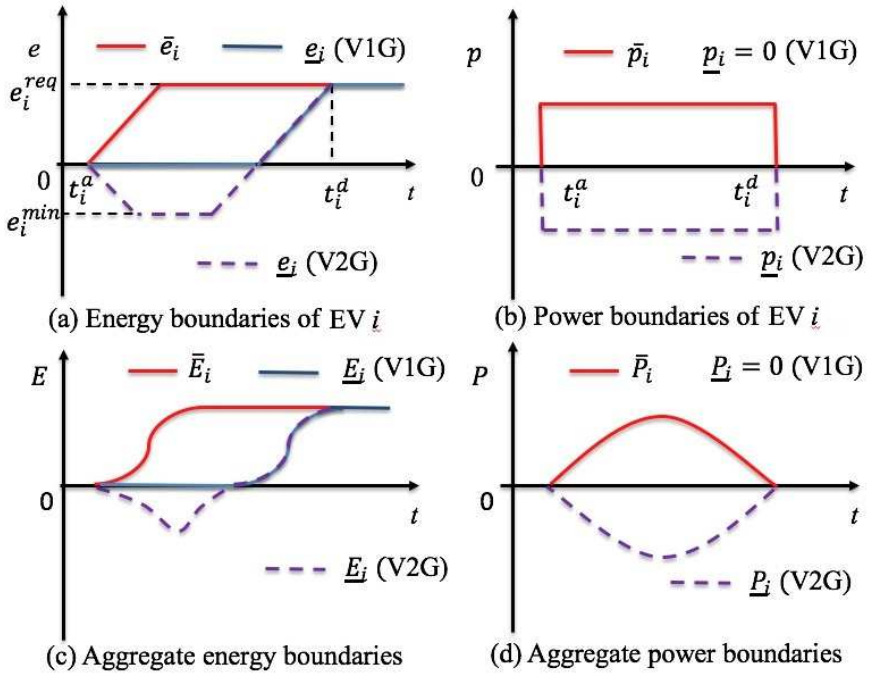

Figure 3. Power and energy boundaries of aggregate battery model

A key challenge here is to estimate the aggregated flexibility of the vehicle fleet. Our essential idea is that the aggregate flexibility can be approximately modeled as a "virtual battery", and it is characterized by the energy and power boundaries of the "virtual battery" [36]. As shown in Figure 3(a)-(b), the flexibility boundaries of the power and energy for EV i are defined as $\{\overline{p}_i,\ \underline{p}_i, \overline{e}_i,\ \underline{e}_i\}$. $\overline{p}_i$ is the maximum charge power and $\underline{p}_i$ is the maximum discharge power. The upper energy boundary $\overline{e}_i$ represents the fastest way to get required energy, while the lower boundary $\underline{e}_i$ is the slowest path. t_i^a represents the arrival time. e_i^{req} is the required energy before departure time t_i^d, and e_i^{min} is the maximum energy discharged during the whole session. Any trajectories within the "envelope" are feasible charging behaviors, because it can guarantee that EV gets required energy before departure without violating battery SOC constraint.

For a collection of EVs, the total power and energy boundaries can be modeled as the summation of individual EVs at any time *t*:

$$\overline{E}_i(t) = \sum_t \overline{e}_i(t), \forall t \tag{4}$$

$$\underline{E}_i(t) = \sum_t \underline{e}_i(t), \forall t \tag{5}$$

$$\overline{P}_i(t) = \sum_t \overline{p}_i(t), \forall t \tag{6}$$

$$\underline{P}_i(t) = \sum_t \underline{p}_i(t), \forall t \tag{7}$$

The Figure 3(c)-(d) shows the boundaries of energy and power for the EV fleet. With the above modeling, a discrete, large-scale formulation is transformed into a smooth, generic and storage-like aggregate model.

3.3. Delivery Optimization Module

After having an accurate estimation on the flexible capacity of EV fleet, it is important to understand the economic benefits of leveraging the flexibility. In this module, we formulate the optimization models for both local services (e.g. tariff optimization, demand charge mitigation, etc.) and grid services (e.g. energy arbitrage, frequency regulation, etc.). The aggregator can decide which service it would like to provide according to the benefits in different markets. If wholesale market is more lucrative, the commitments will be made to the wholesale market. Otherwise, the aggregator will choose to minimize the electricity bills on retail market.

Figure 4 shows the general workflow of optimization process. “Virtual battery” parameters come from capacity availability module. If aggregator decides to provide wholesale market services, then optimization will ingest wholesale electricity market prices of different products. The optimization model maximizes the total revenues by stacking all products together, namely energy, frequency regulation and reserve. Optimization results contain the bidding decisions of each individual product, considering both market level and aggregate battery level constraints. If aggregator decides to focus on local tariff optimization, optimization will take local electricity prices

as inputs and run the two-level optimization model. Upper level aims to minimize the total energy cost with consideration of battery degradation cost. Since the linear model in upper level may have multiple optimal solutions, the lower level aims to find the solution with minimum peak power. The output will be the dispatch profile of aggregate battery.

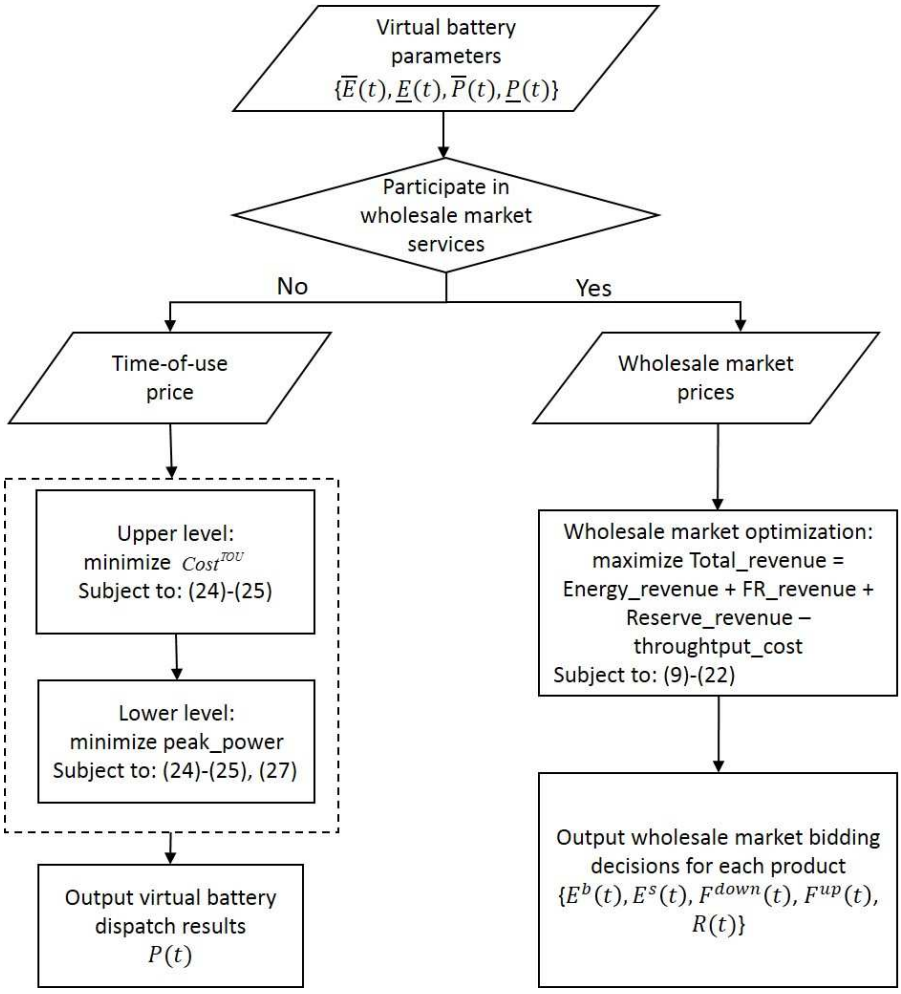

Figure 4. General workflow of optimization process

The detailed optimization formulations are presented as follows:

3.3.1 Wholesale market optimization

(a) Objective function:

$$\begin{aligned}\max \text{Total\_Revenue}=&\text{Energy\_revenue}+\text{FR\_revenue}\\&+\text{Reserve\_revenue}-\text{Throughput\_cost}\end{aligned} \tag{8}$$

where:

$$\text{Energy\_revenue}=\sum_{t=1}^{T}\{[E^{s}(t)-E^{b}(t)]+[F^{up}(t)-F^{down}(t)]\cdot\Delta t\cdot\sigma(t)+R(t)\cdot\Delta t\cdot\omega(t)\}\cdot Price^{energy}(t) \tag{9}$$

$$\text{FR\_revenue}=\sum_{t=1}^{T}[F^{up}(t)*Price^{up}(t)+F^{down}(t)*Price^{down}(t)] \tag{10}$$

$$\text{Reserve\_revenue}=\sum_{t=1}^{T}R(t)*Price^{reserve}(t) \tag{11}$$

$$\text{Throughput\_cost}=\sum_{t=1}^{T}[E^{s}(t)+F^{up}(t)\cdot\Delta t\cdot\sigma(t)+R(t)\cdot\Delta t\cdot\omega(t)]*\varepsilon \tag{12}$$

The objective (8) is to maximize the total revenues from electricity market by stacking all products together. Revenues from energy, frequency regulation, spinning and non-spinning reserve are defined in Equations (9) – (11). Battery throughput cost caused by V2G is modeled in Equation (12) to avoid abusing battery on energy arbitrage. Battery throughput is measured by the total discharge energy from energy sell, frequency regulation up and reserve services.

(b) Constraints:

$$0 \le E^s(t) \le \underline{P}(\mathrm{t}) \cdot \Delta t \cdot \alpha(t), \forall t \in [1,T] \tag{13}$$

$$0 \le E^b(t) \le \overline{P}(\mathrm{t}) \cdot \Delta t \cdot \beta(t), \forall t \in [1,T] \tag{14}$$

$$\alpha(t)+\beta(t) \le 1, \forall t \in [1,T] \tag{15}$$

$$F^{down}(t) \le \overline{P}(t) + \underline{P}(t), \ \forall t \in [1,T] \tag{16}$$

$$F^{up}(t) \le \overline{P}(t) + \underline{P}(t), \ \forall t \in [1,T] \tag{17}$$

$$R(t) \le \underline{P}(t), \ \forall t \in [1,T] \tag{18}$$

$$E^b(t) + F^{down}(t) \cdot \Delta t - F^{up}(t) \cdot \Delta t - E^s(t) - R(t) \cdot \Delta t \le \overline{P}(t) \cdot \Delta t, \forall t \in [1,T] \tag{19}$$

$$E^s(t) + F^{up}(t) \cdot \Delta t - E^b(t) + R(t) \cdot \Delta t \le \underline{P}(t) \cdot \Delta t, \forall t \in [1,T] \tag{20}$$

$$SOE(t) + [E^b(t) \cdot \eta - E^s(t)/\eta] + [F^{down}(t) \cdot \eta - F^{up}(t)/\eta] \cdot \Delta t \cdot \sigma(t) + R(t)/\eta \cdot \Delta t \cdot \omega(h) \le \overline{E}(t+1) \tag{21}$$

$$SOE(t) + [E^b(t) \cdot \eta - E^s(t)/\eta] + [F^{down}(t) \cdot \eta - F^{up}(t)/\eta] \cdot \Delta t \cdot \sigma(t) + R(t)/\eta \cdot \Delta t \cdot \omega(h) \ge \underline{E}(t+1) \tag{22}$$

Battery power constraints are represented in Equations (13) – (15). Energy buy and sell cannot exceed the aggregate battery max charge and discharge power. Constraints (15) guarantees that battery cannot buy and sell energy at the same time. Constraint (16) and (17) model the power constraint on frequency regulation. Frequency regulation bid amount cannot exceed the max power deviation of aggregate battery $\bar{P}(t) + \underline{P}(t)$. Constraint (18) requires that reserve capacity bid does not exceed maximum discharge power. When all products are stacked and co-optimized, market compliance in Equation (19) and (20) require that battery charge or discharge from all products should stay

within battery power limits. Battery energy dynamics are modeled in Equations (21)-(22). It makes sure that remaining energy of aggregate battery always stays within the required energy boundaries calculated in battery availability module.

In this formulation, we have two binary variables which avoid to bid buy and sell at the same time. Continuous variables represent the bidding amount for each products, including $\{E^b(t), E^s(t), F^{down}(t), F^{up}(t), R(t)\}$. Since they are all time dependent, the total number of variables in the simulation depends on the optimization horizon.

3.3.2 Local tariff optimization

In the retail market, the risk of price volatility has been covered by the load serving entity [47]. EV owner is charged at contracted tariff (e.g. TOU price). On top of that, demand charge is also widely adopted by utility companies to limit the load peak of commercial and industrial customers, such as shopping malls, office buildings, parking lots and etc. Shifting charge load from peak hours to off-peak hours can effectively reduce the electricity cost. At the same time, it is also important to make sure the concentrate charging will not cause new load peaks which may result in high demand charges. Thus, the optimization can be divided to two-levels. For the upper level, the aggregator aims to reduce the total charging cost $Cost^{TOU}$:

$$\min Cost^{TOU} = \sum_{t \in T} P(t) \cdot \Delta t \cdot \lambda(t) + P(t) \cdot \Delta t \cdot \varepsilon \tag{23}$$

subject to:

$$\underline{P}(t) \le P(t) \le \overline{P}(t) \tag{24}$$

$$\underline{E}(t) \le P(t) \cdot \Delta t + \sum_{\tau=1}^{t-1} P(\tau) \cdot \Delta t \le \overline{E}(t) \tag{25}$$

The first part of Equation (23) represents the total electricity cost. The second part is the cost of battery degradation caused by extra discharge for energy arbitrage. The aggregate power and energy constraints are shown in Equation (24) and (25). By solving this problem, the aggregator can find the minimum cost charging schedule.

The lower level is described as:

$$\min \max P(t),\ t \in [1, 2, ..., T] \tag{26}$$

subject to constraints (24)-(25), and:

$$\sum_{t \in T} P(t) \cdot \Delta t \cdot [\lambda(t) + \varepsilon] = Cost^{min,TOU} \tag{27}$$

The target of the lower level in Equation (26) is to reduce the charging/discharging peak power during the scheduled period. The lower level optimization still needs to meet the energy and power constraints (24)-(26). On top of that, constraint (27) requires that the solution from second stage also achieves the minimum cost $Cost^{min,TOU}$ from the upper level. In this formulation, the only decision variable is battery power $P(t)$. Since it is time dependent, the number of variables is proportional to the optimization horizon.

3.4. Resource Allocation Module

In Delivery Optimization Module, the aggregator makes the aggregate power commitments based on the forecasting information on EV travel patterns and market prices. The total power commitments need to be disaggregated and dispatched to individual vehicles at the real-time stage, i.e. the aggregator must decide how much charge/discharge power to allocate to each vehicle. This real-time control or scheduling problem is a central algorithmic challenge faced by the aggregator. The aggregator has to perform the allocation under the uncertainties from both EV and system status. There are a few heuristic control strategies that can be explored including Earliest Deadline First (EDF) or Least Laxity First (LLF) [48]. EDF allocates power to EVs prioritized by their anticipated departure time, while LLF allocates power prioritized by the charging demands [49]. The real-time control algorithm for allocating and dispatching vehicles fundamentally affects the feasibility and value proposition of VGI.

Allocating energy to each individual EV requires the controller to know the exact session parameters, including the start time t_i^s and the stay duration d_i, as well as the energy consumption value e_i. In addition, enough energy is supposed to be delivered to each individual EV before its deadline t_i^d, i.e. the departure time of the EV i. In the real-world scenario, however, we cannot assume perfect insights on itineraries. For each EV, the battery energy constraints and charging power are formulated with itinerary uncertainties as follows:

$$0 \le p_i(t) \le \bar{p}, \forall t \in [t_i^s, t_i^s + \hat{d}_i] \tag{28}$$

$$e_i(t) = e_i(t - \Delta t) + p_i(t) \cdot \Delta t, \forall t \in [t_i^s, t_i^s + \hat{d}_i] \tag{29}$$

$$\hat{e}_i \le e_i(t_i^s + \hat{d}_i) \le e_B \tag{30}$$

where $p_i(t)$ represents the instant charging power for EV i at time t; $\bar{p}$ is the maximum charging rate of the charging infrastructure. Note that, the departure time of EV i is replaced with $t_i^s + \hat{d}_i$, where $\hat{d}_i$ is the estimated parking duration from a real-time predictor. Equation (29) describes the increment of stored energy in the battery of each individual EV. The stop criteria for each EV, i.e. Equation (30), is to get more energy than the estimated value $\hat{e}_i$, while less than the total battery capacity e_B.

Given the optimal aggregate charging load profile from the Delivery Optimization Module, the real-time allocation aims to reduce the cumulative gap between the desired and real load profiles. Thus, the objective of the charging power allocation problem is formulated as:

$$\min \sum_{t=\tau}^{T} [\sum_{i=1}^{I} p_i(\tau) - \hat{P}(\tau)]^2 \tag{31}$$

subject to constraints (28) – (30).

As the EVs number increases, the centralized controller has to: i) collect the timely measurements for all EVs; ii) compute the optimal charging schedules; and then iii) send control signals to each individual charging facility. Compared with decentralized controller, it has some practical drawbacks, including: 1) user privacy issue, i.e. related

information for all users has to be collected altogether by the centralized server; 2) high computation burden and communication network condition may delay the delivering of the optimal charging schedules. Instead, in decentralized approaches, each individual EV computes its own optimal charging schedules, without knowing schedule information of other EVs. EVs send their updated charging schedules to a server asynchronously and get updated control/price signals back until all EVs reach an equilibrium state. We deploy the decentralized algorithms developed in our previous paper in this module [50]. We extend the scheduling algorithm to follow aggregate EV charging load profile and add another layer of iterations to simulate the real-time operations, i.e. predictively optimize the energy consumption schedules in each time step given estimated session parameters for each EV, and then implement only the first element in the charging schedule (the next time step). The detailed decentralized strategy is as follows:

a) For aggregator

In each iteration k, the aggregator or system operator needs to calculate the consensus-based control signal, i.e. c_k^τ, as follows:

$$c_k^\tau = \frac{1}{\gamma} \cdot [\sum_{i=1}^{I} p_i^k(\tau) - \hat{P}(\tau)] \tag{32}$$

where $\hat{P}(\tau)$ is the optimal charging load at time τ from the first-stage planning and $\gamma$is a Lipschitz constant.

b) For each EV

Each EV solves the following local optimization problem given its estimated itinerary and the energy demand values, as well as the updated control signal c_k^τ from the system operator.

$$\min \sum_{t=\tau}^{T} c_k^\tau \cdot p_i(t) + \sum_{t=\tau}^{T} [p_i^{k-1}(\tau) - p_i^k(\tau)]^2 \tag{33}$$

subject to constraints (28) - (30).

The optimality and convergence proof for this algorithm has been provided in [50]. The detailed simulation flow can be found in Appendix I.

3.5. Value Estimation Module

This is an ex-post evaluation function. After the real-time allocation, the earnings for providing different services are calculated, also the battery degradation and operating cost. Penalties will be liquidated by evaluating the deviation between dispatch signal and the real-time performance.

4. Simulation and Case Study

4.1. Simulation setup

The proposed framework and methods are developed into a simulation toolkit in Python 3.8 [51]. The optimization problems are formulated in cvxpy [52], and solved by Gurobi 9.1 optimization solver [53]. Simulations were performed on a PC with Intel Core™ i7 CPU@3.20 GHz and 128GB RAM. The optimization environment is set up as same as the literature [54].

All reported results are obtained by studying a collection of 10,000 EVs. EV travel itineraries are randomly extracted from National Household Travel Survey (NHTS) dataset [55]. We also use a common TOU rate (PGE E-9 [56]) for EV charging in California, USA to verify the performance of local tariff optimization in 3.3.2. Since VGI values in wholesale electricity market heavily rely on market structure and prices, we perform studies on both CAISO [57] and ERCOT [58] with prices of year 2018.

The proposed solution supports flexible setting of input parameters, e.g. time step, simulation period (from one day to multiple years), market prices, etc. In the following sections, we use single-day results to give an in-depth analysis on the simulation flow and detailed battery dispatch behavior. Whole year simulation results follow to provide comprehensive understanding on the economic savings from VGI and computational performance of the proposed tool.

4.2. Simulation Results

4.2.1. Single day analysis

As we discussed in Section 3.1, the EV estimation module firstly takes NHTS travel itineraries as inputs. Driving cycles are automatically generated according to the average speed. Detailed trip chain will track energy consumption and battery status in a second-by-second basis. This module will also generate individual level constraints, which is used in following optimization problems.

The aggregate flexibility is represented by power and energy boundaries. As shown in the top plot of Figure 5, the energy upper bound is the charging as soon as possible path.

The cumulative energy consumption should not exceed the upper bound at any time. The energy lower bound is the charging as late as possible path. It defines the minimum accumulative energy required by the EVs at any time. In this case, vehicles will start from discharging and wait until the last minute to start charging in order to reach the required SOC before leaving. Any cumulative trajectories between the upper bound and low bound are valid charging path, which can guarantee all vehicles have enough energy for traveling and avoid exceeding their maximum capacities. The power boundaries are decided by charging facilities. In this study, we assume two levels of charging power: L1 (1.44kW) at home and L2 (6.6kW) at workplaces. As shown in the bottom plot of Figure 5, the power range between 8:00-17:00 are wide, because most of EVs park at workplaces which have L2 chargers. The energy and power boundaries will work together as important constraints in the following optimization. Since we aggregate all the power and energy constraints as two constraints, it will significantly reduce the computational time.

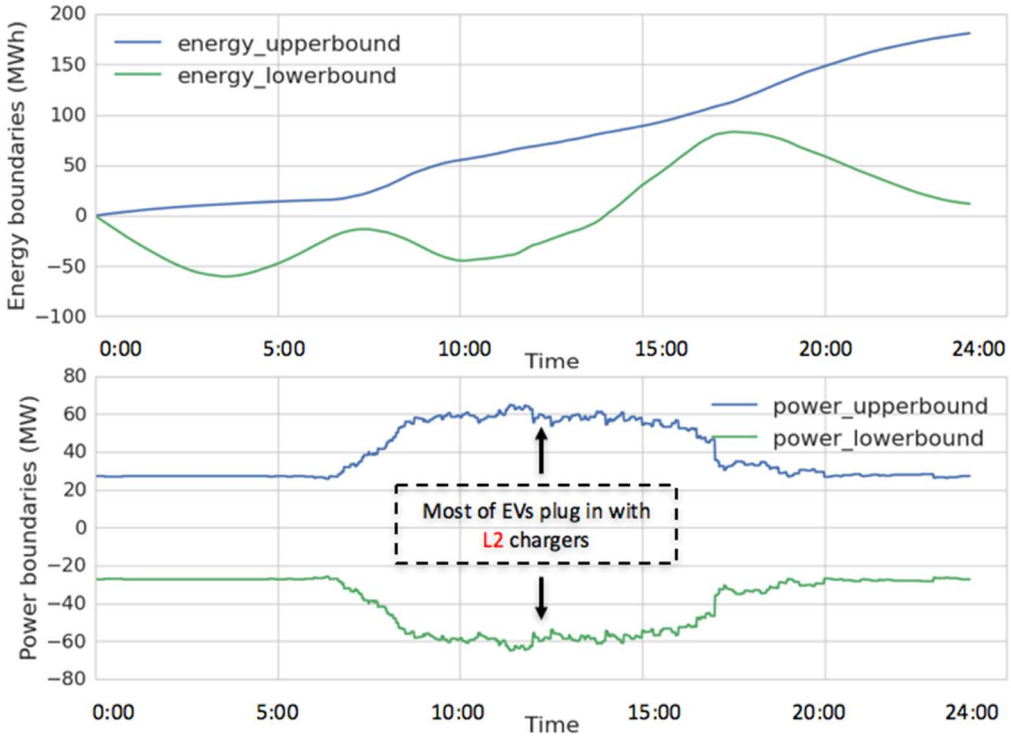

Figure 5. Aggregate flexibility of 10,000 EVs.

The delivery optimization module decides which market the aggregator would participate in. If the aggregator provides wholesale market services, the module will solve the wholesale market optimization problem in 3.3.1. Energy and ancillary service related costs are estimated based on historical data. Figure 6(a) shows the bidding results of no battery degradation scenario. Energy arbitrage happens in most hours. The aggregator purchases energy during lower price time and selling energy out to get revenues. Regulation up and down services only happen on 18:00 and 22:00-24:00. There are two reasons: (1) The price of frequency regulation and spinning reserve is relatively low; (2) Since the dispatch signal may be less than 1, even if the aggregator bid

for ancillary services, it can only earn the capacity payment, but not the benefits from selling net energy. Compared with the certain benefits from energy arbitrage, ancillary services are uncertain. If we consider the battery degradation cost 0.16$/kWh, since the battery degradation cost is larger than the price difference between peak and valley, no energy sale happens as shown in Figure 6 (b). The aggregator bids on regulation up and down according to the forecasting information.

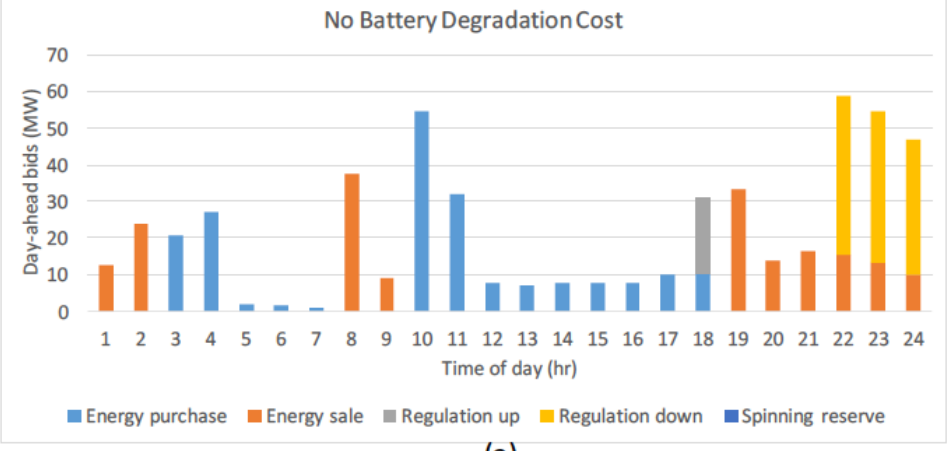

(a)

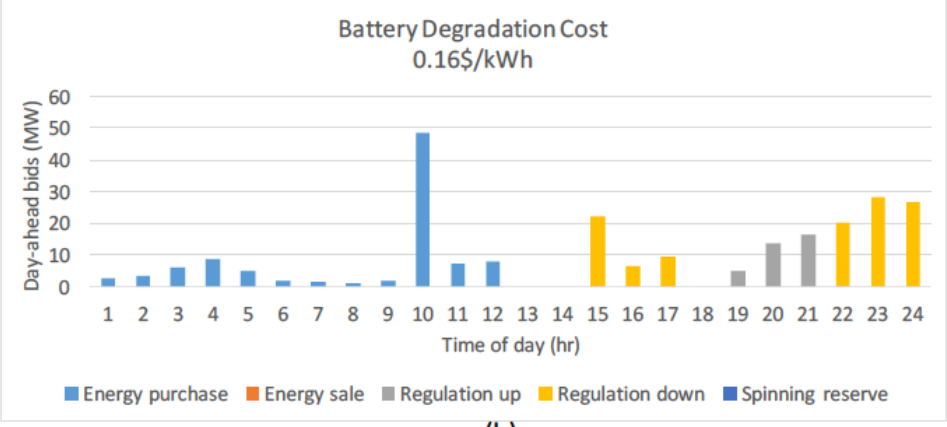

(b)

Figure 6. Bidding results at wholesale market: (a) no battery degradation cost scenario; (b) 0.16$/kWh battery degradation cost scenario.

Since the wholesale market prices are relatively low, the aggregator may normally choose to provide retail level services. The formulations (20) – (24) provide a solution for aggregator to minimize the total energy cost under TOU price, at the same time mitigate the demand charge. As shown in Figure 7, we compared three charging scenarios. As to the uncontrolled charging scenario, all vehicles begin to be charged once they arrive at workplace or home. The charging operation lasts until the battery is charged to full or the vehicle leaving. As depicted in Figure 7, there are two peaks on uncontrolled charging load curve. The first one happens around 8:00 am, when most of vehicles arrive at workplaces and start charging. The second one happens around 18:00, when EVs get home. In this case, EV owners does not consider the charging prices. In the minimum cost charging case, the vehicle will avoid charging the battery during peak time. During wintertime, there are two levels of prices: peak and partial-peak. Peak time is from 5:00pm -8:00pm. The rest is partial peak time. As shown in in Figure 7, from 17:00 – 20:00, load would be shifted to other periods to avoid peak price. Some vehicles have to charge to get enough energy, even though the price is high. After the price recovers to off-peak time, there is a high load spike. It may cause high demand charge and harm the grid. Using the two-stage algorithm would avoid this problem. It can be seen that without increasing charge cost under TOU price, the charging load is leveled during the whole scheduling horizon. The load peak is reduced by 20% compared to uncontrolled case and 90% compared to minimum cost case.

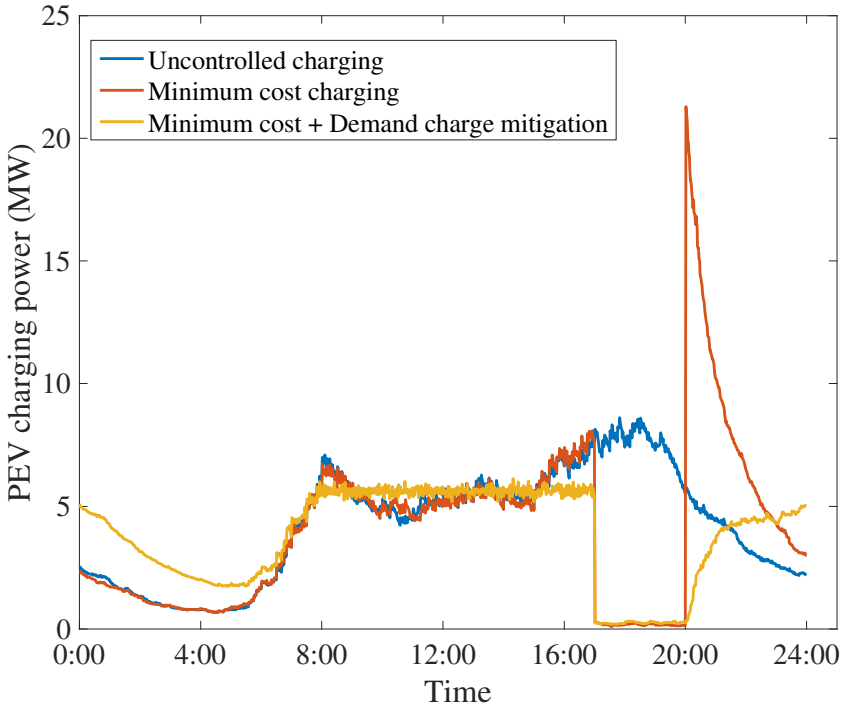

Figure 7. Results on retail market service.

After getting the optimal lead time commitment, the total committed aggregate power should be allocated to each individual vehicle at the real time. Resource Allocation Module allows aggregation entities to determine how individual vehicle resources should be dispatched to meet aggregate commitments after ensuring to meet the driving needs of each vehicle first. The inputs are the forward commitments made by an aggregator, the reference signals that must be followed at run-time (e.g. AGC signals), and the constraints of individual vehicles. The outputs are the dispatch commands to EVs according to the unique control strategy chosen by aggregator.

In the real time, there are uncertainties from both dispatch signal and EV behavior. At each time step in the simulation, a random noise is added to the parked duration and the energy demand value for each EV. As shown in Figure 8, we compare the allocation performance between LLF and proposed predictive method. The dispatch signal is a combined hourly signal of bulk energy, frequency regulation and spinning reserve. It is obvious that predictive control algorithm follows the dispatch signal better than the LLF. If we define the accumulative mismatch as equation (34):

$$M = \int_{t=1}^{T} |U(t) - D(t)| \delta t \tag{34}$$

where M is the cumulative mismatch in MWh, $U(t)$ is the real delivery at time t, $D(t)$ is the dispatch signal at time t. The total mismatch from LLF is 99.39MWh, while the mismatch between dispatch signal and predictive control is 46.34MWh.

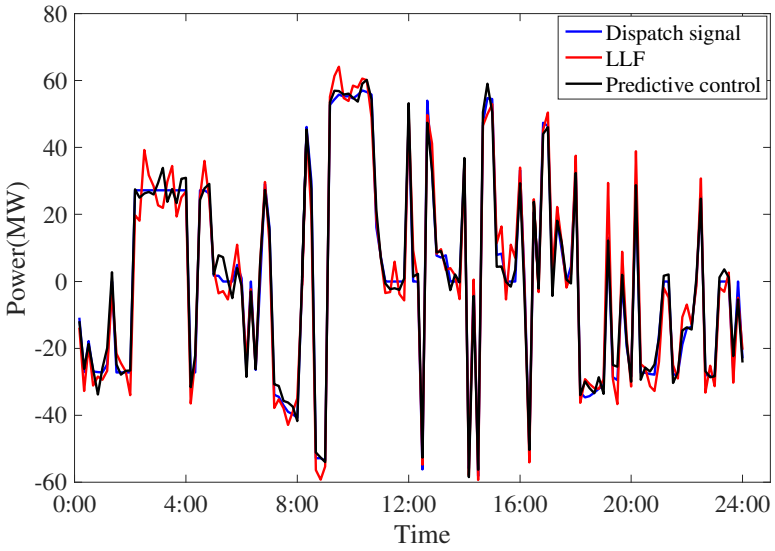

Figure 8. Resource Allocation Module

After the real-time allocation, all information including benefits, costs and penalties have been determined. The value estimation module will perform an ex-post evaluation. When the vehicles perform retail level services, the total charging cost under uncontrolled charging scenario is $18919.4. Using the proposed algorithm can reduce the energy cost by 18.3%. Since the peak is reduced by 20%. The demand charge cost over the month is reduced by 29.3%. In this tariff, the demand charge rate is 17.56$/kW. In wholesale market, we use the energy and ancillary service prices of CAISO market on a 7/1/2015 as shown in figure in the Appendix II. In the uncontrolled charging case, the total cost is $1778. Following the bidding strategy describe in Figure 6, the total cost can be brought down to $1,205. The detailed costs and benefits are shown in Table 3.

Table 3. Output from value estimation module

Market	Cost	Uncontrolled（$）	Proposed（$）
Retail level	Energy cost	18,919.4	15,445
	Demand charge	151,121	106,870
Wholesale level	Total cost	1,778	1,205

4.2.2. Annual results

In order to provide a comprehensive understanding on the economic value of VGI and computational performance of the proposed solution, we extended the simulation to whole year period. Driving patterns are randomly sampled from NHTS dataset and then

fed into EV estimation module. Power and energy boundaries of the aggregate battery $\{\overline{E}(t), \underline{E}(t), \overline{P}(t), \underline{P}(t)\}$ are calculated from capacity availability module over the course of a year. In the delivery optimization module, we use wholesale market prices of year 2018 from CAISO and ERCOT to quantify the VGI values in different electricity markets. The retail tariff is PG&E E-9 TOU rate, which is the same as what is shown in single-day simulation.

Economic benefits from local tariff optimization are shown in Table 4. We compare the energy costs and demand charges between uncontrolled charging and proposed bi-level optimized charging strategies. Whole-year simulation shows that energy cost is reduced by 20.6% and demand charge is reduced by 33.8%, if we use the bi-level optimization. The total electricity bill decreases by 24.4%. Figure 9 shows the monthly breakdown results. Both demand charge and energy charge are reduced consistently over months. It should be noted that we are not seeing strong seasonal patterns here, mainly because we only simulate EV charging load. Demand charge is normally measured by the highest 15-min peak load of each month for the entity. Co-optimizing EV charging load along with base load of the entity to reduce demand charge is beyond the scope of this paper.

Table 4. Economic values from local tariff optimization

Strategy	Energy charge ($)	Demand charge ($)	Total electricity bill ($)

Uncontrolled charging	5,594,411	2,210,939	7,805,350
Bi-level optimization	4,439,712	1,463,234	5,902,946

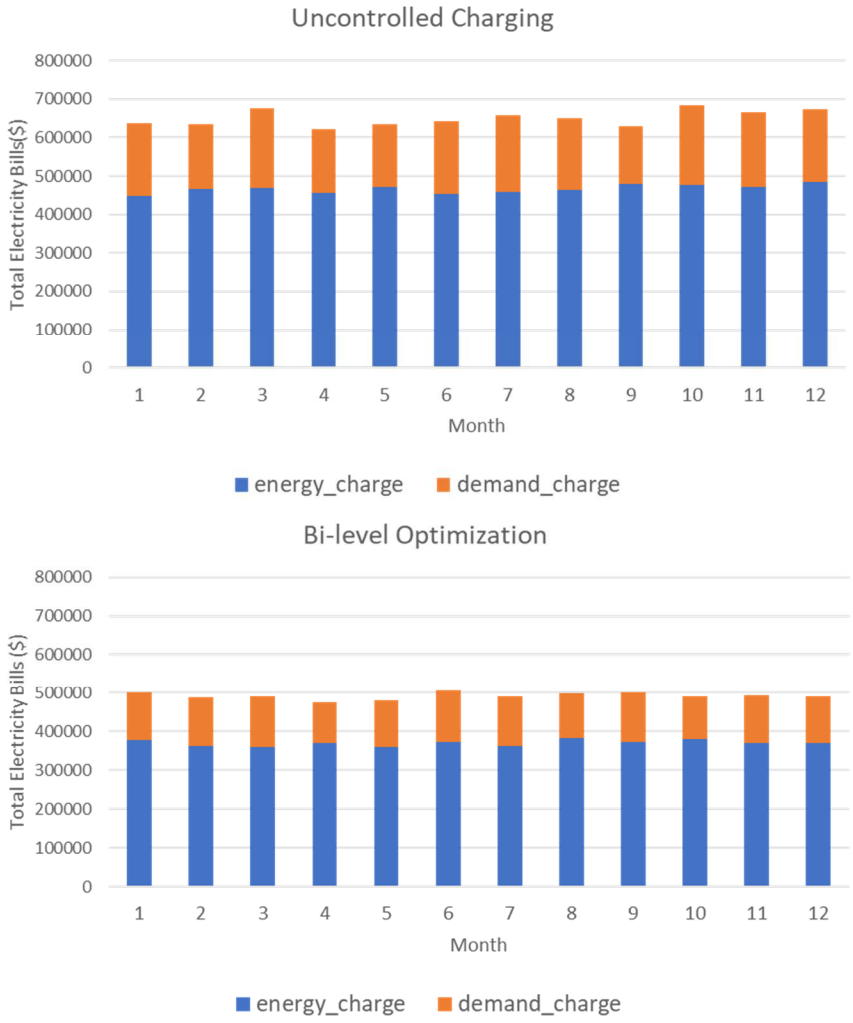

Figure 9. Monthly breakdown electricity bills from "uncontrolled charging" vs. "bi-level optimization"

In order to quantify VGI values in different wholesale electricity markets, we ran the portfolio optimization model in 3.2.1 with price data of year 2018 from both CAISO and ERCOT markets. The revenues from all products are shown in Table 5. We also list some statistics of year 2018 prices from these two markets in Table 6 to help understand the results. We can see that values varies between these two markets and among different products. Since ERCOT generally has lower energy price and higher volatility, the energy cost in ERCOT is 35% lower than that in CAISO. In this simulation, we assume battery throughput cost is 0.16$/kWh, so energy arbitrage is discouraged except extreme high price events. Most of revenues come from frequency regulation and reserve products. Frequency regulation is more lucrative than reserve in CAISO, while reserve accounts for most of revenues ERCOT. Table 5 shows the max reserve price even hits 7,000 $/MW in ERCOT. It is worth to mention that energy conversation ratio of reserve product is generally low, which means aggregator can get payment for the capacity reserve most of time without discharging much energy to the grid. The total annual revenues in ERCOT is 2.7 times of what is achieved in CAISO.

Table 5. Economic values from wholesale market optimization

Electricity market	Revenue($)			
	Energy	Frequency Regulation	Reserve	Total
CAISO	-877,259	1,938,698	1,487,459	2,548,898
ERCOT	-569,197	582,151	6,897,321	6,910,276

Table 6. Statistics of CAISO and ERCOT market prices in year 2018

Market	Product	mean	std	min	median	max
CAISO	Energy ($/MWh)	38.0	31.2	-24.7	33.7	921.4
	Reg_up ($/MW)	10.9	21.3	0.1	7.3	723.6
	Reg_down ($/MW)	10.3	10	0	7.8	119.4
	Reserve ($/MW)	6.8	20.8	0.1	3.0	716.6
ERCOT	Energy ($/MWh)	30.2	55.0	4.4	23.6	2058.0
	Reg_up ($/MW)	9.1	12.8	0	5.8	150
	Reg_down ($/MW)	5.7	8.1	0	3.5	150
	Reserve ($/MW)	14.0	85.2	0.8	8.5	7,000

The above results are based on 160$/MWh battery throughput cost (degradation cost). However, there is a clear trend that battery cost will keep decreasing over years. Battery throughput cost is a key parameter that has big impact on VGI values in wholesale electricity market. With the proposed framework, we can easily perform sensitivity analysis on throughput cost. Figure 10 shows the annual revenues from CAISO and ERCOT markets with different throughput costs. We can see the ERCOT revenue slopes is flat when the throughput cost is higher than 60$/MWh. It is because most revenues come from reserve product, which is mainly from capacity payment without requiring delivery much energy in real time. Revenues reach the upper bound when throughput

cost is 0. The upper bound in ERCOT is $8,476,559 and in CAISO is $4,998,076. If we distribute revenues to individual EVs evenly, it will be $848/year in ERCOT and $500/year in CAISO.

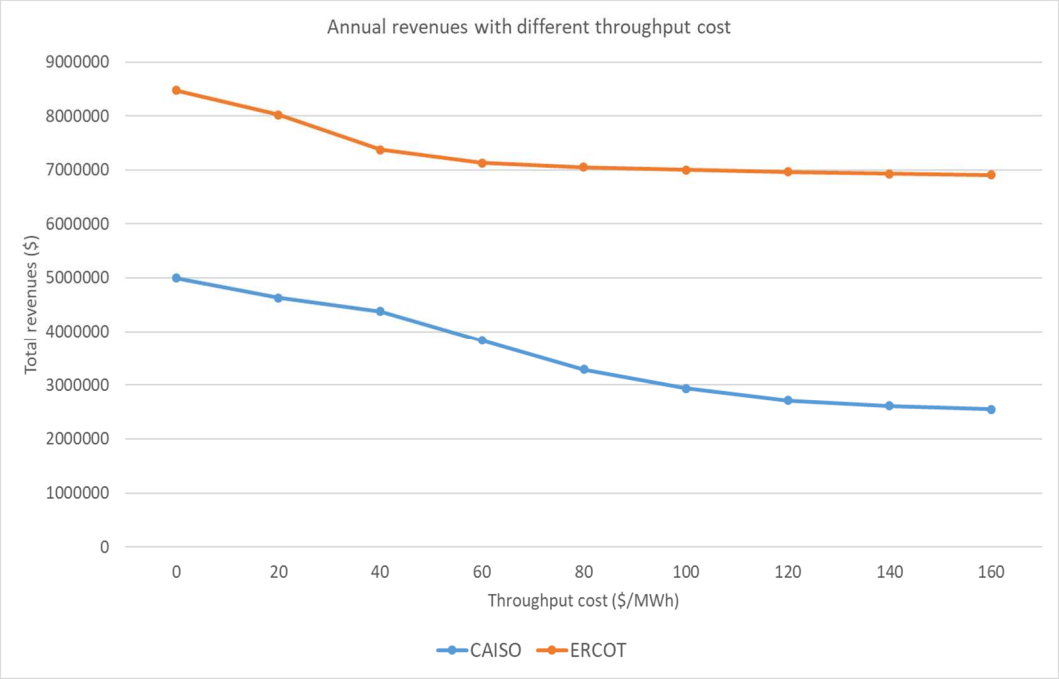

Figure 10. Annual revenues from CAISO and ERCOT with different throughput cost

Optimization model sizes and execution times in different use cases are presented in Table 7. One year simulations in both use cases take less than 16 minutes. The retail level optimization does bi-level iteration, therefore it creates some overhead on computational time. It is worth to call out here that model size is irrelevant to number of EVs, since we use the “aggregate battery model”. To be specific, the computational time is reduced by ~10,000 times, compared to the scenario of optimizing each EV independently.

Table 7. Optimization number of variables

Use case	Number of variables	Equations	Computational time (s)
Local tariff optimization	17,520	78,840	723
Wholesale market optimization	61,320	87,600	932

5. Conclusions

In this paper, we develop an integrated simulation framework to quantify economic values of vehicle grid integration. Five sub-modules cover the whole process from estimating individual EV energy consumption to evaluating the final monetary values of providing grid services. Optimization models are formulated for both wholesale market participation and local level charging cost management. A predictive control strategy is used to solve the energy allocation problem in a decentralized manner. We use a 10,000-EV case study to demonstrate the functionalities of the proposed framework. Interpretation of the outputs leads to the main conclusions as follows:

(1) This paper firstly presents a “virtual battery” model to quantify the aggregate flexibility of EV fleet, which is described by power and energy boundaries. The aggregated model changes the discrete distributed individual charging need into a stable and smooth aggregated model, therefore, increases the reliability of scheduling strategy. Moreover, the aggregate model significantly reduce the number of variables in

optimization problems, compared to the scenario in which each individual EV's constraints are modeled.

(2) A bi-level optimization is proposed to reduce EV energy cost by shifting charge demand based on TOU rate, while avoid increasing demand charge peaks. Simulation results show that energy cost is reduced by 20.6% and demand charge is reduced by 33.8%, compared to the uncontrolled charging.

(3) A wholesale market optimization model is built to maximize VGI values by stacking all products together, including energy, frequency regulation and reserve. The proposed framework is flexible to take prices from the wholesale electricity market which is of interest, and provide detailed dispatch results for each individual product. Simulation results show that the fleet achieves 2.7 times of revenues from ERCOT market than CAISO market based on price data of year 2018. Because of very spiky reserve price in ERCOT market, the fleet can still achieve decent revenues (~$691 per EV per year) although with a conservative assumption on battery throughput cost at 0.16$/kWh.

(4) Sensitivity analysis on battery throughput cost indicates that more values from frequency regulation and energy arbitrage can be unlocked as throughput cost continues to decrease.

(5) Compared with classic centralized control methods, the proposed predictive method can greatly enhance the real-time allocation performance, reduce the computational burden and alleviate the communication delay.

Acknowledgements

This work was supported with funding from the Department of Energy Vehicle Technologies Office, under the Grid Modernization Lab Consortium.

Appendix

Appendix I. Predictive & Decentralized EV Management Strategy

Aggregate level optimization:

Solve the problems in Delivery Optimization Module.

Real-time resource allocation:

For $\tau = 1$ *to* T

Retrieve the aggregate charging profile $\hat{P}(\tau), \hat{P}(\tau+1), \cdots, \hat{P}(T)$;

Do

Initialize a random charging schedule for each EV, i.e. $p_i^0(t_i^s), p_i^0(t_i^s+1), \cdots, p_i^0(t_i^s+\hat{d}_i)$;

Iteration count $k = 0$;

Operator: calculate c_k^τ, using Equation (32);

For $i = 1{:}I$

Estimate the updated stay duration $\hat{d}_i$ and energy demand $\hat{e}_i$;

Each EV: solve Equation (30) for updated schedule, i.e. $p_i^k(t_i^s), p_i^k(t_i^s+1), \cdots, p_i^k(t_i^s+\hat{d}_i)$, subject to constraints (28) - (30);

End For

$k = k + 1$;

$error = \|c_k^\tau - c_{k-1}^\tau\|$;

While $error > erro\_min$

For $i = 1{:}I$

Implement $p_i(\tau)$, if $t_i^s \le \tau < t_i^s + \hat{d}_i$

End for

End for

Appendix II California Energy and Ancillary Service Price on 7/1/2015

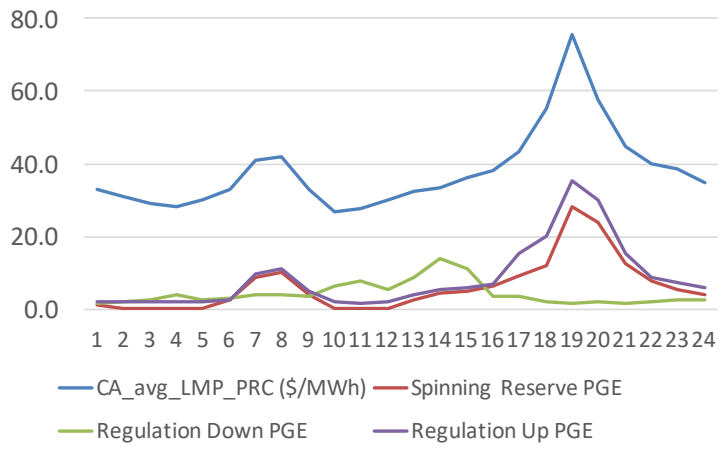

References

[1] J. Williams et al., "The technology path to deep greenhouse gas emissions cuts by 2050: The pivotal role of electricity," Science, vol. 336, no. 6079, pp. 296-296, 2012, doi: 10.1126/science.1208365.

[2] L. Barelli, G. Bidini, D. A. Ciupăgeanu, C. Pianese, P. Polverino, and M. Sorrentino, "Stochastic power management approach for a hybrid solid oxide fuel cell/battery auxiliary power unit for heavy duty vehicle applications," Energy Conversion and Management, vol. 221, pp. 113197, Oct. 2020, doi: 10.1016/j.enconman.2020.113197.

[3] "Newsroom | Governor Edmund G. Brown Jr." [Online] Available: https://www.ca.gov/archive/gov39/newsroom/index.html, accessed 22 Jul, 2020.

[4] C. Zhang, J. B. Greenblatt, P. MacDougall, S. Saxena, and A. Jayam Prabhakar, "Quantifying the benefits of electric vehicles on the future electricity grid in the midwestern United States," Applied Energy, vol. 270, pp. 115174, Jul. 2020, doi: 10.1016/j.apenergy.2020.115174.

[5] Z. A. Needell, J. McNerney, M. T. Chang et al., "Potential for widespread electrification of personal vehicle travel in the United States," Nature Energy, vol. 1, no. 9, pp. 1-7, 2016, doi: 10.1038/nenergy.2016.112.

[6] S. Saxena, J. MacDonald, and S. Moura, "Charging ahead on the transition to electric vehicles with standard 120 V wall outlets," Applied Energy, vol. 157, pp. 720–728, Nov. 2015, doi: 10.1016/j.apenergy.2015.05.005.

[7] C. Zhang, D. Wang, B. Wang, and F. Tong, "Battery Degradation Minimization-Oriented Hybrid Energy Storage System for Electric Vehicles," Energies, vol. 13, no. 1, pp. 246, Jan. 2020, doi: 10.3390/en13010246.

[8] N. Nezamoddini and Y. Wang, "Risk management and participation planning of electric vehicles in smart grids for demand response," Energy, vol. 116, pp. 836–850, Dec. 2016, doi: 10.1016/j.energy.2016.10.002.

[9] D. Wang, X. Guan, J. Wu, P. Li, P. Zan, and H. Xu, "Integrated energy exchange scheduling for multimicrogrid system with electric vehicles," IEEE Transactions on Smart Grid, vol. 7, no. 4, pp. 1762–1774, Jul. 2016, doi: 10.1109/TSG.2015.2438852.

[10] H. Fathabadi, "Novel wind powered electric vehicle charging station with vehicle-to-grid (V2G) connection capability," Energy Conversion and Management, vol. 136, pp. 229–239, Mar. 2017, doi: 10.1016/j.enconman.2016.12.045.

[11] Global EV Outlook 2020, n.d. [Online] Available: https://www.iea.org/publications/reports/ globalevoutlook2020/

[12] Members|Zev Alliance, n.d [Online] Available: http://www.zevalliance.org/members

[13] EV Sales Forecasts – EVAdoption, n.d [Online] Available: https://evadoption.com/ev-sales/ev-sales-forecasts/

[14] C. F. Heuberger, P. K. Bains, and N. Mac Dowell, "The EV-olution of the power system: A spatio-temporal optimisation model to investigate the impact of electric vehicle deployment," Applied Energy, vol. 257, pp. 113715, 2020, doi: 10.1016/j.apenergy.2019.113715.

[15] S. Rangaraju, L. De Vroey, M. Messagie et al., "Impacts of electricity mix, charging profile, and driving behavior on the emissions performance of battery electric vehicles: A Belgian case study," Applied Energy, vol. 148, pp. 496-505, 2015, doi: 10.1016/j.apenergy.2015.01.121.

[16] N. E. Koltsaklis, and A. S. Dagoumas, "Incorporating unit commitment aspects to the European electricity markets algorithm: An optimization model for the joint clearing of energy and reserve markets," Applied energy, vol. 231, pp. 235-258, 2018, doi: 10.1016/j.apenergy.2018.09.098.

[17] M. Muratori, "Impact of uncoordinated plug-in electric vehicle charging on residential power demand," Nature Energy, vol. 3, no. 3, pp. 193-201, 2018, doi: 10.1038/s41560-017-0074-z.

[18] X. Li et al., "A cost-benefit analysis of V2G electric vehicles supporting peak shaving in Shanghai," Electric Power Systems Research, vol. 179, pp. 106058, Feb. 2020, doi: 10.1016/j.epsr.2019.106058.

[19] K. E. Forrest, B. Tarroja, L. Zhang, B. Shaffer, and S. Samuelsen, "Charging a renewable future: The impact of electric vehicle charging intelligence on energy storage requirements to meet renewable portfolio standards," Journal of Power Sources, vol. 336, pp. 63–74, Dec. 2016, doi: 10.1016/j.jpowsour.2016.10.048.

[20] B. Tarroja, L. Zhang, V. Wifvat, B. Shaffer, and S. Samuelsen, "Assessing the stationary energy storage equivalency of vehicle-to-grid charging battery electric vehicles," Energy, vol. 106, pp. 673–690, Jul. 2016, doi: 10.1016/j.energy.2016.03.094.

[21] E. C. Kara, J. S. Macdonald, D. Black, M. Bérges, G. Hug, and S. Kiliccote, "Estimating the benefits of electric vehicle smart charging at non-residential locations: A data-driven approach," Applied Energy, vol. 155, pp. 515–525, Oct. 2015, doi: 10.1016/j.apenergy.2015.05.072.

[22] K. Clement-Nyns, E. Haesen, and J. Driesen, "The impact of charging plug-in hybrid electric vehicles on a residential distribution grid," IEEE Transactions on Power Systems, vol. 25, no. 1, pp. 371–380, Feb. 2010, doi: 10.1109/TPWRS.2009.2036481.

[23] S. M. Mousavi Agah and A. Abbasi, "The impact of charging plug-in hybrid electric vehicles on residential distribution transformers," in Iranian Conference on Smart Grids, pp. 1–5, May 2012,

[24] S. I. Vagropoulos, D. K. Kyriazidis, and A. G. Bakirtzis, "Real-time charging management framework for electric vehicle aggregators in a market environment," IEEE Transactions on Smart Grid, vol. 7, no. 2, pp. 948-957, 2015, doi: 10.1109/TSG.2015.2421299.

[25] H. Fathabadi, "Utilizing solar and wind energy in plug-in hybrid electric vehicles," Energy Conversion and Management, vol. 156, pp. 317–328, Jan. 2018, doi: 10.1016/j.enconman.2017.11.015.

[26] B. K. Sovacool, J. Kester, L. Noel, and G. Zarazua de Rubens, "Actors, business models, and innovation activity systems for vehicle-to-grid (V2G) technology: A

comprehensive review," Renewable and Sustainable Energy Reviews, vol. 131, p. 109963, Oct. 2020, doi: 10.1016/j.rser.2020.109963.

[27] E. Sortomme and M. A. El-Sharkawi, "Optimal combined bidding of vehicle-to-grid ancillary services," IEEE Transactions on Smart Grid, vol. 3, no. 1, pp. 70–79, Mar. 2012, doi: 10.1109/TSG.2011.2170099.

[28] S. I. Vagropoulos and A. G. Bakirtzis, "Optimal bidding strategy for electric vehicle aggregators in electricity markets," IEEE Transactions on Power Systems, vol. 28, no. 4, pp. 4031–4041, Nov. 2013, doi: 10.1109/TPWRS.2013.2274673.

[29] R. Mehta, D. Srinivasan, A. M. Khambadkone et al., "Smart charging strategies for optimal integration of plug-in electric vehicles within existing distribution system infrastructure," IEEE Transactions on Smart Grid, vol. 9, no. 1, pp. 299-312, 2016, doi: 10.1109/TSG.2016.2550559.

[30] C. Le Floch, F. Belletti, and S. Moura, "Optimal charging of electric vehicles for load shaping: A dual-splitting framework with explicit convergence bounds," IEEE Transactions on Transportation Electrification, vol. 2, no. 2, pp. 190–199, Jun. 2016, doi: 10.1109/TTE.2016.2531025.

[31] L. Gan, U. Topcu, and S. H. Low, "Optimal decentralized protocol for electric vehicle charging," IEEE Transactions on Power Systems, vol. 28, no. 2, pp. 940-951, 2012, 10.1109/tpwrs.2012.2210288.

[32] W. Kempton and J. Tomić, "Vehicle-to-grid power implementation: From stabilizing the grid to supporting large-scale renewable energy," Journal of Power Sources, vol. 144, no. 1, pp. 280–294, Jun. 2005, doi: 10.1016/j.jpowsour.2004.12.022.

[33] A. Schuller, C. M. Flath, and S. Gottwalt, "Quantifying load flexibility of electric vehicles for renewable energy integration," Applied Energy, vol. 151, pp. 335–344, Aug. 2015, doi: 10.1016/j.apenergy.2015.04.004.

[34] R. Shi, S. Li, P. Zhang, and K. Y. Lee, "Integration of renewable energy sources and electric vehicles in V2G network with adjustable robust optimization," Renewable Energy, vol. 153, pp. 1067–1080, Jun. 2020, doi: 10.1016/j.renene.2020.02.027.

[35] B. Zhang and M. Kezunovic, "Impact on Power System Flexibility by Electric Vehicle Participation in Ramp Market," IEEE Transactions on Smart Grid, vol. 7, no. 3, pp. 1285–1294, May 2016, doi: 10.1109/TSG.2015.2437911.

[36] H. Zhang, Z. Hu, Z. Xu et al., "Evaluation of achievable vehicle-to-grid capacity using aggregate PEV model," IEEE Transactions on Power Systems, vol. 32, no. 1, pp. 784-794, 2016, doi: 10.1109/TPWRS.2016.2561296.

[37] D. Wang, J. Gao, P. Li, B. Wang, C. Zhang, and S. Saxena, "Modeling of plug-in electric vehicle travel patterns and charging load based on trip chain generation," Journal of Power Sources, vol. 359, pp. 468–479, Aug. 2017, doi: 10.1016/j.jpowsour.2017.05.036.

[38] J. Hernández, F. Sanchez-Sutil, F. Muñoz-Rodríguez et al., "Optimal sizing and management strategy for PV household-prosumers with self-consumption/sufficiency enhancement and provision of frequency containment reserve," Applied Energy, vol. 277, pp. 115529, 2020, doi: 10.1016/j.apenergy.2020.115529.

[39] M. Gomez-Gonzalez, J. C. Hernandez, D. Vera et al., "Optimal sizing and power schedule in PV household-prosumers for improving PV self-consumption and providing frequency containment reserve," Energy, vol. 191, pp. 116554, 2020, doi: 10.1016/j.energy.2019.116554.

[40] J. Hernández, F. Sanchez-Sutil, and F. Muñoz-Rodríguez, "Design criteria for the optimal sizing of a hybrid energy storage system in PV household-prosumers to maximize self-consumption and self-sufficiency," Energy, vol. 186, pp. 115827, 2019, doi: 10.1016/j.energy.2019.07.157.

[41] J. Coignard, S. Saxena, J. Greenblatt et al., "Clean vehicles as an enabler for a clean electricity grid," Environmental Research Letters, vol. 13, no. 5, pp. 054031, 2018, doi: 10.1088/1748-9326/aabe97.

[42] C. Zhang, J. B. Greenblatt, P. MacDougall et al., "Quantifying the benefits of electric vehicles on the future electricity grid in the midwestern United States," Applied Energy, vol. 270, pp. 115174, 2020, doi: 10.1016/j.apenergy.2020.115174.

[43] A. Rousseau et al., "Electric Drive Vehicle Development and Evaluation Using System Simulation," IFAC Proceedings Volumes, vol. 47, no. 3, pp. 7886–7891, 2014, doi: 10.3182/20140824-6-ZA-1003.02832.

[44] O. US EPA, "Dynamometer Drive Schedules," US EPA, Sep. 16, 2015 [Online] Available: https://www.epa.gov/vehicle-and-fuel-emissions-testing/dynamometer-drive-schedules, accessed 22 Jul, 2020.

[45] D. Wang, J. Coignard, T. Zeng et al., "Quantifying electric vehicle battery degradation from driving vs. vehicle-to-grid services," Journal of Power Sources, vol. 332, pp. 193-203, 2016, doi: 10.1016/j.jpowsour.2016.09.116.

[46] B. Wang, R. Yin, and D. Black, "Comprehensive Modeling of Electric Vehicles in California Demand Response Markets," Apr. 2018, Accessed: Jul. 22, 2020. [Online]. Available: https://arxiv.org/abs/1804.02580v1.

[47] S. Bae, H. Zhang, D. Wang, C. Sheppard, and S. Saxena, "Optimal bidding strategy for V2G regulation services under uncertainty," in 2017 IEEE Power Energy Society General Meeting, pp. 1–5, Jul. 2017, doi: 10.1109/PESGM.2017.8274706.

[48] J. Hong, X. Tan, and D. Towsley, "A performance analysis of minimum laxity and earliest deadline scheduling in a real-time system," IEEE Transactions on Computers, vol. 38, no. 12, pp. 1736–1744, Dec. 1989, doi: 10.1109/12.40851.

[49] A. Subramanian, M. J. Garcia, D. S. Callaway et al., "Real-time scheduling of distributed resources," IEEE Transactions on Smart Grid, vol. 4, no. 4, pp. 2122-2130, 2013, doi: 10.1109/TSG.2013.2262508.

[50] B. Wang, Y. Wang, H. Nazaripouya et al., "Predictive scheduling framework for electric vehicles with uncertainties of user behaviors," IEEE Internet of Things Journal, vol. 4, no. 1, pp. 52-63, 2016, https://ieeexplore.ieee.org/document/7590111.

[51] Python 3.8 [Online] Available: https://www.python.org/downloads/release/python-380/

[52] cvxpy [Online] Available: https://www.cvxpy.org/

[53] Gurobi 9.1 optimization solver [Online] Available:https://www.gurobi.com/products/gurobi-optimizer/

[54] K. Seddig, P. Jochem, and W. Fichtner, "Two-stage stochastic optimization for cost-minimal charging of electric vehicles at public charging stations with photovoltaics," Applied energy, vol. 242, pp. 769-781, 2019. 3, doi: 10.1016/j.apenergy.2019.03.036

[55] "National Household Travel Survey." Available: https://nhts.ornl.gov/, accessed 22 Jul, 2020.

[56] "Tariffs." [Online] Available: https://www.pge.com/tariffs/index.page, accessed 22 Jul, 2020.

[57] CAISO [Online] Available: http://www.caiso.com/Pages/default.aspx

[58] ERCOT [Online] Available: http://www.ercot.com/